Pure appl. geophys. 161 (2004) 623–646
0033–4553/04/030623–24
DOI 10.1007/s00024-003-2466-1

Pure and Applied Geophysics

Seismic Sources on the Iberia-African Plate Boundary and their Tectonic Implications

E. BUFORN[1], M. BEZZEGHOUD[2], A. UDÍAS[1], and C. PRO[3]

Abstract—The plate boundary between Iberia and Africa has been studied using data on seismicity and focal mechanisms. The region has been divided into three areas: A; the Gulf of Cadiz; B, the Betics, Alboran Sea and northern Morocco; and C, Algeria. Seismicity shows a complex behavior, large shallow earthquakes ($h < 30$ km) occur in areas A and C and moderate shocks in area B; intermediate-depth activity ($30 < h < 150$ km) is located in area B; the depth earthquakes ($h \approx 650$ km) are located to the south of Granada. Moment rate, slip velocity and *b* values have been estimated for shallow shocks, and show similar characteristics for the Gulf of Cadiz and Algeria, and quite different ones for the central region. Focal mechanisms of 80 selected shallow earthquakes ($8 \geq m_b \geq 4$) show thrust faulting in the Gulf of Cadiz and Algeria with horizontal NNW-SSE compression, and normal faulting in the Alboran Sea with E-W extension. Focal mechanisms of 26 intermediate-depth earthquakes in the Alboran Sea display vertical motions, with a predominant plane trending E-W. Solutions for very deep shocks correspond to vertical dip-slip along N-S trends. Frohlich diagrams and seismic moment tensors show different behavior in the Gulf of Cadiz, Betic-Alboran Sea and northern Morocco, and northern Algeria for shallow events. The stress pattern of intermediate-depth and very deep earthquakes has different directions: vertical extension in the NW-SE direction for intermediate depth earthquakes, and tension and pressure axes dipping about 45 ° for very deep earthquakes. Regional stress pattern may result from the collision between the African plate and Iberia, with extension and subduction of lithospheric material in the Alboran Sea at intermediate depth. The very deep seismicity may be correlated with older subduction processes.

Key words: Plate boundary, Iberia-African, seismicity, focal mechanisms, intermediate and deep depth earthquakes, subduction.

Introduction

The interaction between Iberia and Africa results in a complex region located in the western part of the Eurasian-African plate boundary. This region corresponds to the transition from an oceanic boundary (between the Azores and the Gorringe Bank), to a continental boundary where Iberia and Africa meet. The plate boundary is very well delimited in the oceanic part, from the Azores Islands along the Azores-Gibraltar fault to approximately 12°W (west of the Strait of Gibraltar). From 12°W

[1] Dpt. de Geofísica, Universidad Complutense, Madrid, Spain.
[2] Dpt. de Física. Universidade de Evora and CGE, Evora, Portugal.
[3] Dpt. de Física, Universidad de Extremadura, Spain.

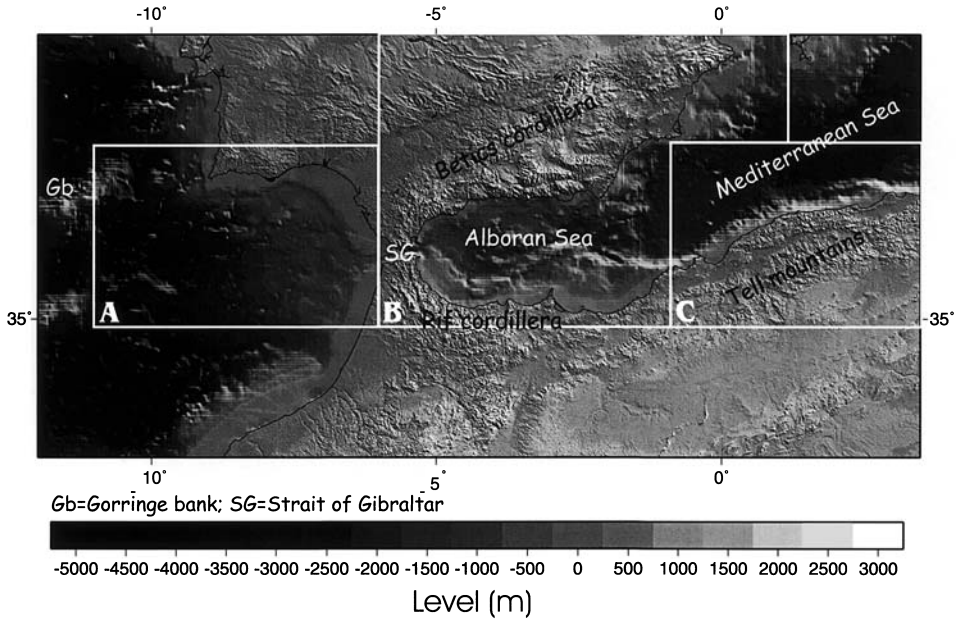

Figure 1
Topography and bathymetry of the Iberia-African region.

to 3.5°E, including the Iberia-African region and extending to the western part of Algeria, the boundary is more diffuse and forms a wider area of deformation (BUFORN *et al.*, 1988a; MOREL and MEGHRAOUI, 1996; HAYWARD *et al.*, 1999).

The complexity of the region is reflected in its bathymetry, seismicity, stress regime and tectonics. In Figure 1 bathymetry and topography for this region are shown. On land, the main geological features are the Betics, the Rif Cordilleras and the Tell Mountains, formed basically by the Alpine domain, a consequence of the collision between Eurasia and Africa. The bathymetry shows, as main features, the Gorringe Bank region, located west of the Strait of Gibraltar, with a number of seamounts, banks and submarine ridges, and the Alboran Sea east of the Strait of Gibraltar, with important regional crustal thickness variations (TORNÉ *et al.*, 2000).

Plate kinematic models for the region have estimated convergence rates of 4mm/yr at the Gorringe Bank and Gibraltar, and 6 mm/yr in the Algerian region (ARGUS *et al.*, 1989; DEMETS *et al.*, 1990), and 7.6 mm/yr in northwestern Algeria from seismic slip rate (LAMMALI *et al.*, 1997). From west to east along the plate boundary between Eurasia and Africa, the general stress pattern corresponds to extension in the Azores region, right-lateral strike-slip motion in the central part and compression in the eastern region, from Gorringe Bank to the Strait of Gibraltar and Algeria (MCKENZIE, 1972; UDÍAS *et al.*, 1976; GRIMISON and CHEN, 1986; BUFORN *et al.*, 1988a; JIMENEZ-MUNT *et al.*, 2001; NEGREDO *et al.*, 2002).

In this paper we have divided the Iberia-African plate boundary region into three areas: A (Gulf of Cadiz to Gorringe Bank), B (central part including Betic and Rif Cordilleras and the Alboran Sea) and C (northwest Algeria and Tell Mountains). We will examine the different characteristics of these three areas using observations of seismicity and focal mechanisms.

Shallow Earthquakes

Seismicity of the Iberia-African region is characterized by the occurrence of earthquakes of moderate magnitude, most of them with focus at shallow depth ($0 < h < 40$ km). The distribution of epicenters corresponding to magnitude $m_b \geq 3.5$, taken from the Instituto Geográfico Nacional Data File (IGN Data File) for the period 1980–1999, is shown in Figure 2. Magnitudes in the IGN Data File have been determined using Lg waves adjusted to values of m_b (BOLETÍN DE SISMOS PRÓXIMOS, 1989). Most shocks correspond to shallow events with magnitudes, in general, less than 5.5. For the 1980–1999 time period, only one earthquake has magnitude greater than 6.0 (El Asnam, Algeria, earthquake 10.10.1980; $M_s = 7.3$). West of Gibraltar, from the Gulf of Cadiz to the Gorringe bank region (area A), epicenters are distributed in an E-W direction, across a band about 100-km wide, with foci at shallow and intermediate depth (Fig. 2). Before the period represented in Figure 2, two large earthquakes had occurred in this region, one in the Gulf of Cádiz (15.3.1964; $M_s = 6.4$) and another west of the San Vicente Cape (29.2.1969; $M_s = 8$)

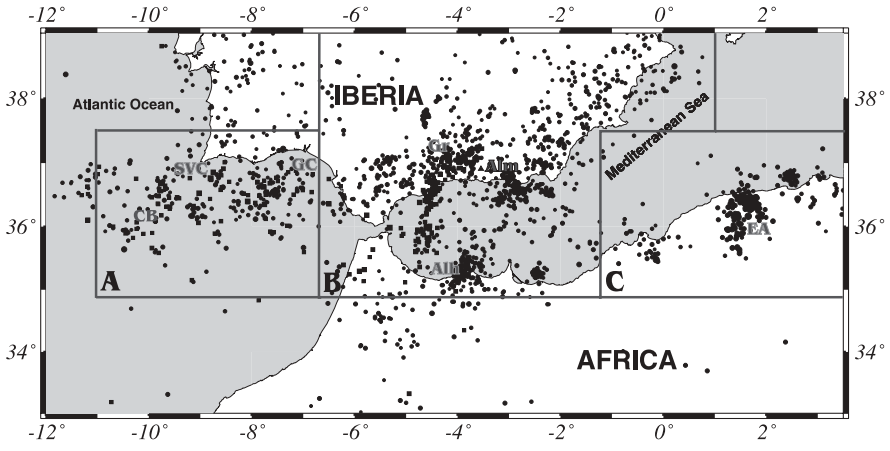

Figure 2
Distribution of epicenters for the period 1980–1999 ($m_b \geq 3.5$) taken from the IGN Data File. Circles correspond to shallow earthquakes ($h < 40$ km), squares to intermediate depth ($40 < h < 150$ km) and triangles to very deep ($h > 600$ km). GB = Gorringe Bank, SVC = San Vicente Cape, GC = Gulf of Cádiz, Gr = Granada, Alm = Almería, ALH = Alhoceima; EA = El Asnam.

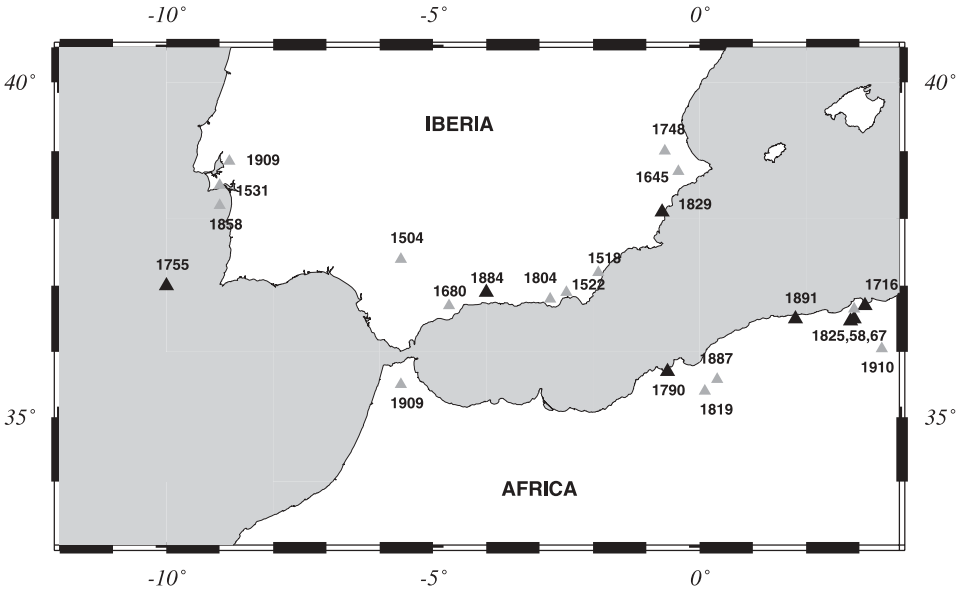

Figure 3
Historical seismicity for the studied region. In black earthquakes with maximum intensity = X, in grey maximum intensity = IX.

(UDÍAS *et al.*, 1976; BUFORN *et al.*, 1988b). In area B there are three main concentrations of epicenters, at 4°W (the Alhoceima region, northern Morocco), where in 1994 an earthquake of magnitude $M_w = 5.8$ occurred (CALVERT *et al.*, 1997; BEZZEGHOUD and BUFORN, 1999); at 2.5°W in the Almeria region (SE Spain) where a swarm occurred in 1993–1994 with two shocks of magnitudes 5.0 (RUEDA *et al.*, 1996), and at 4.5°W in the Granada Basin with frequent shocks of m_b about 3. In area C shocks are concentrated in the El Asnam region, Algeria, at 2°E, where earthquakes with $M_s > 6$ occurred in 1954 ($M_s = 6.5$) and 1980 ($M_s = 7.3$).

Historical seismicity (shocks with maximum intensity of IX or X, occurring between 1500 and 1910 for the region are represented in Figure 3 (MÉZCUA and MARTINEZ SOLARES, 1983; MUÑOZ and UDÍAS, 1988; MOKRANE *et al.*, 1994). Larger earthquakes (Io = X) are located west of S. Vicente Cape (Lisbon earthquake, 1755), southern Iberia (1829 and 1884) and northeastern Algeria (1716, 1790, 1825, 1858 and 1891). In northern Morocco only one large earthquake has occurred with maximum intensity IX in 1909. In Spain, except for the earthquake of 1504 (Carmona, Sevilla), shocks are located very near the coast in the south and southeast. Another area of high activity is the Lower Tajo Valley, near Lisbon, Portugal.

A selection of focal mechanisms for shallow earthquakes in this region taken from previous studies, together with four new solutions estimated in this study (Annex 1), are shown in Figure 4 and Table 1. Criteria used for the selection of the

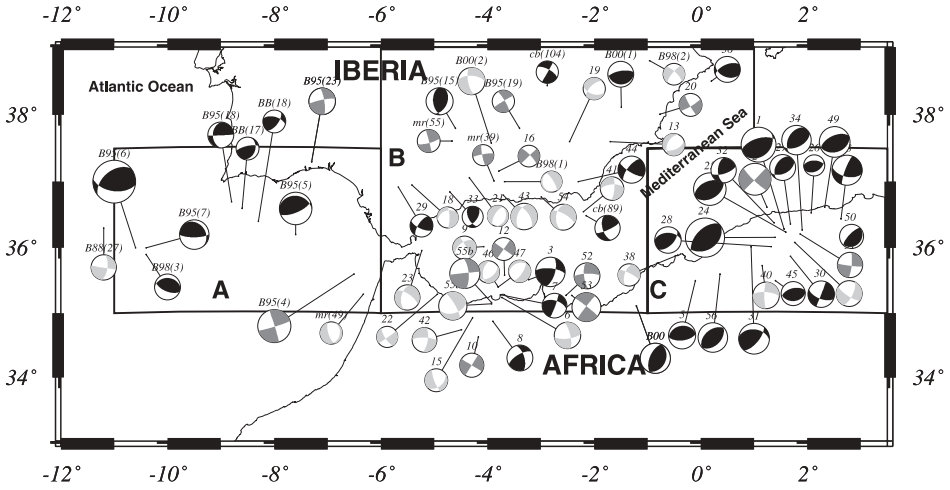

Figure 4
Focal mechanisms for shallow earthquakes (h < 40 km) and $m_b \geq 5.0$, before 1975 and $m_b \geq 4.0$ after 1975. In black thrusting solutions, in dark grey strike-slip and in grey normal solutions. Size is proportional to magnitude. Numbers correspond to Table 1.

solutions are: $m_b \geq 5$ for shocks that occurred before 1975, and $m_b \geq 4$ for shocks after 1975. The new solutions are based on more than 15 polarity data, and nodal planes are well defined. Six solutions were obtained from modelling or inversion of body waves and the rest from polarities of *P* waves. This selection of focal mechanisms has been chosen so that the solutions represent the regional stress pattern, and the local effects present in smaller earthquakes are avoided.

From Figure 4 we observe that fault plane solutions show predominantly thrusting motion in areas A and C (Gulf of Cadiz and Algeria regions), with an average horizontal compression in the NNW-SSE direction. There exist some strike-slip mechanisms in A (events B95 (4), B95 (23)) and in B (events 2, 51, 40), which are also compatible with a horizontal compression in the NNW-SSE direction. For these earthquakes tension axes are also horizontal in the NNE-SSW direction. Strike-slip solutions have a predominantly E-W plane with right-lateral motion, the northern block moving east. In area B (central region) focal mechanisms show a greater variety of solutions. Solutions correspond to normal faulting (5), strike-slip mechanisms with a large component of normal motion (10), reverse faulting (4), strike-slip with a large component of reverse motion (7), and pure strike-slip faulting (15). Thus a normal component of motion is present in 15 shocks. In this respect area B differs from A and C, where the predominant motion is of reverse character. Most solutions in area B are compatible with a stress pattern consisting of a general horizontal tension axis in the E-W direction and a horizontal pressure axis in the NW-SE direction. Solutions with a large normal component and vertical *P* axis are more frequent on the south coast of Spain and in the Alboran Sea.

Table 1

Solutions for focal mechanisms of shallow earthquakes represented in Figure 4. ϕ: strike, δ: dip, λ: slip. NF is the reference plotted with each solution

Date	Lat. N	Long.E	Depth	M	ϕ	δ	λ	NF	Ref.
190551	37.58	−3.93	30	5.1	169	69	−35	B00(2)	9
090954	36.28	1.57	10	6.5	253	61	104	1	1
100954	36.62	1.24	30	6.0	44	90	−8	2	1
230859	35.51	−3.23	20	5.5	276	70	153	3	1
051260	35.60	−6.50	15	6.2	73	86	−178	B95(4)	2
150364	36.2	−7.60	12	6.1	*276	24	117	B95(5)	2
130767	35.50	−0.10	5	5.1	260	30	87	5	1
170468	35.24	−3.73	22	5.0	83	70	−162	6	1
301068	35.28	−3.76	5	4.6	286	55	145	7	1
280269	36.10	−10.60	22	8.0	231	47	54	B95(6)	2
050569	36.00	−10.40	29	5.5	324	24	142	B95(7)	2
070470	34.87	−3.90	5	4.8	244	64	151	8	1
180472	36.30	−11.20	15	4.7	8	65	−2	B88(27)	7
221172	36.02	−4.07	5	4.4	234	50	−15	9	1
290473	34.63	−4.17	10	4.5	212	90	1	10	1
140774	35.58	−3.68	5	4.3	305	90	180	12	1
060677	37.60	−1.70	10	4.2	208	45	−121	13	1
150777	35.17	−3.73	13	4.0	211	70	−25	14	1
240279	34.93	−4.28	5	4.3	51	40	−23	15	1
200379	37.16	−3.79	5	4.1	316	78	−179	16	1
210479	35.03	−4.00	5	4.0	173	71	148	17	1
010579	36.95	−5.42	24	4.0	249	35	−24	18	1
140579	37.70	−2.46	5	4.2	107	49	−40	19	1
251079	38.01	−0.77	20	4.3	59	81	−7	20	1
221279	37.06	−4.34	40	4.0	210	64	−86	21	1
100280	35.29	−4.94	5	4.0	55	85	−18	22	1
220680	35.96	−5.93	30	4.7	304	66	−135	23	1
101080	36.16	1.39	5	7.3	*225	54	83	24	1
101080	36.24	1.59	10	6.1	58	43	81	25	1
131080	36.53	2.07	5	4.0	63	42	69	26	1
301080	36.26	1.68	5	4.8	210	46	64	27	1
081180	36.02	1.32	5	5.0	270	45	126	28	1
031280	36.92	−5.67	27	4.3	114	68	155	29	1
051280	35.87	1.68	5	5.0	112	61	−179	30	1
071280	36.02	0.94	5	5.8	277	40	140	31	1
150181	36.38	1.38	8	4.7	181	53	29	32	1
210181	36.85	−4.71	5	4.0	153	56	46	33	1
010281	36.27	1.90	11	5.5	210	43	64	34	1
140281	36.08	1.76	26	4.9	26	67	−18	35	1
050381	38.50	0.20	5	4.9	113	42	128	36	1
200381	35.13	−3.90	5	4.0	164	89	133	37	1
190481	35.89	−0.43	16	4.2	198	57	−16	38	1
070481	35.12	−3.98		4.0	182	75	132	39	1
151182	35.73	1.15	7	5.0	274	70	−169	40	1
060183	36.49	−2.15	12	4.7	163	58	14	cb(89)	3
200383	36.55	−2.20	6	4.4	266	62	−18	41	1
241183	34.74	−4.49	40	4.6	272	74	−23	42	1
240684	36.80	−3.70	5	5.0	201	48	−46	43	1

Table 1 (contd.)

Date	Lat. N	Long.E	Depth	M	ϕ	δ	λ	NF	Ref.
130984	37.00	−2.30	9	5.1	121	73	156	44	1
100485	38.43	−2.88	5	4.2	298	67	−3	cb(104)	3
030585	35.50	1.40		4.5	225	54	83	45	1
260585	37.80	−4.60	5	5.1	174	51	70	B95(15)	2
201086	36.70	−8.80	37	4.8	180	37	3	B95(18)	2
110387	37.80	−3.40	7	4.2	329	80	2	B95(19)	2
091287	35.40	−3.82	14	4.2	54	49	−58	46	1
051088	35.40	−3.80	11	4.2	248	26	−58	47	1
311088	36.44	2.63	13	5.7	103	55	167	48	1
051288	37.01	−3.88	5	4.0	169	82	73	mr(39)	6
291089	36.61	2.33	31	5.8	242	55	87	49	1
201289	37.30	−7.30	23	5.0	351	77	10	B95(23)	2
090290	36.26	2.83	18	4.5	49	18	95	50	1
071190	37.00	−3.68	2	4.0	165	16	−74	B98(1)	9
150691	35.90	−10.40	6	4.8	273	30	73	B98(3)	9
140891	38.80	−0.96	4	4.1	314	72	−164	B98(2)	9
190192	36.21	1.86	4	4.7	277	85	−169	51	1
120392	35.27	−2.53	8	4.8	268	76	−161	52	1
160293	36.60	−8.60	26	4.3	17	33	34	BB(17)	5
010593	35.29	−6.33	30	4.2	15	25	−60	mr(49)	6
230593	35.27	−2.42	6	5.4	308	86	4	53	1
220693	36.40	−8.30	15	4.3	37	62	40	BB(18)	5
231293	36.77	−2.99	8	4.9	300	70	−130	54	1
260594	35.14	−3.92	7	5.3	*330	77	−45	55a	1
260594	35.16	−3.92	8	5.7	*355	79	2	55b	1
180894	35.60	0.36	4	5.7	*58	45	95	56	1
160496	37.61	−4.66	8	4.3	75	76	−179	mr(55)	6
020299	38.11	−1.49	5	4.8	260	67	89	B00(1)	4
221299	35.26	−1.45	6	5.6	*25	31	92	B00	8

1. BEZZEGHOUD and BUFORN. (1999); 2. BUFORN *et al.* (1995); 3. COCA and BUFORN (1994); 4. BUFORN and SANZ DE GALDEANO (2001); 5. BORGES *et al.* (2001); 6. MEZCUA and RUEDA (1997); 7. BUFORN *et al.* (1988a); 8. YELLES-CHAOUCHE *et al.*, This issue; 9. This paper; *Modeling or inversion of body waves.

Intermediate Depth Earthquakes

Important seismic activity at intermediate depth ($150 > h > 40$ km) is present in parts A and B, as can be seen in Figure 2 (MUNUERA, 1963; HATZFELD, 1978; GRIMISON and CHENG, 1986; BUFORN *et al.*, 1988b, 1991a, b, 1997; SEBER *et al.*, 1996; SERRANO *et al.*, 1998). This activity is shown in more detail for the period 1980–1999 and $m_b \geq 3.5$, in Figure 5 (I.G.N. Data File). The reliability of depth determinations for this time period was improved by the installation of the network of the IGN in Spain (Tejedor and García, 1993). Magnitudes m_b of earthquakes in this figure are between 3.5 and 5. In part A, intermediate-depth shocks are spread over a band approximately 100-km wide, (between 36°N and 37°N), extending E-W from 8°W to 11°W. The most important concentration of foci at intermediate depth

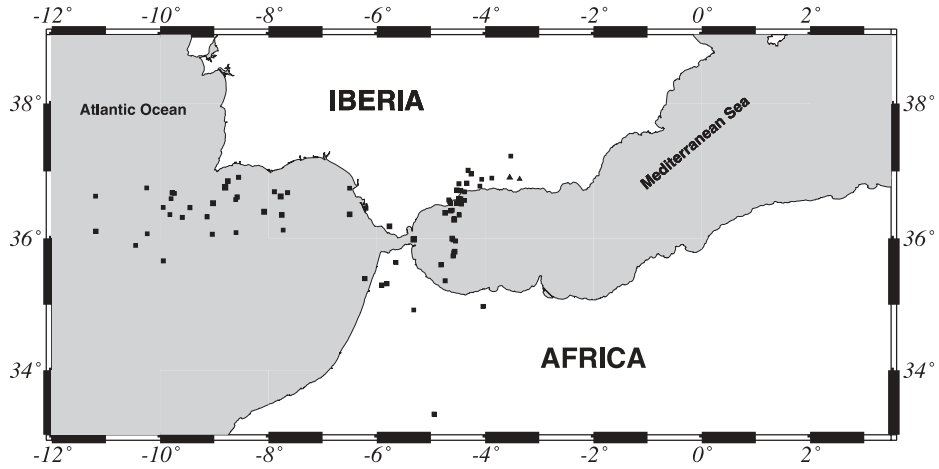

Figure 5
Distribution of epicenters at intermediate depth (40 < h < 150 km, squares) and very deep earthquakes (h > 600 km, triangles). The period represented is 1980–1999 (Instituto Geográfico Nacional, Data File).

is in part B, at the eastern side of the Strait of Gibraltar in a narrow N-S trending band less than 50-km wide, centered at 4.5°W and extending from 35°N to 37°N. Thus the distribution of intermediate-depth shocks differs in area A (E-W trend) from that of area B (N-S trend). No intermediate depth seismic activity is observed east of 3°W in Spain, Morocco or Algeria.

A vertical E-W cross section of the seismicity, showing the distribution of hypocenters along a band between 12°W and 2°W and centered at 36°N, is shown in Figure 6a. From this figure we observe that most earthquakes in part A have depths less than about 60 km. In part B, at about 4.5°W there is a concentration of shocks to depths of 100 km in a very narrow band of less than 50 km. To the east of this area depths decrease rapidly with maximum depths less than 40 km to the east of 3°W (to Algeria). No intermediate-depth activity is found in part C.

Figures 6b and 6c show N-S vertical cross sections along bands centered at longitudes 9°W (Gulf of Cadiz) and 4.5°W (western part of the Alboran Sea). For the Gulf of Cadiz (Fig. 6b), most earthquakes occur at depths less than 60 km, with most foci concentrated between latitudes 36°N and 37°N. In the Alboran Sea (Fig. 6c) depths increase to values around 100 km, with an important concentration of hypocenters between 60 and 100 km occurring between latitudes 35°N and 37°N. These shocks correspond to the narrow band in Figure 6a. There is an apparent gap between 30 and 50 km for the same latitudes however this may be due to the crustal model used in the hypocentral determinations.

Focal mechanisms for 27 selected intermediate-depth events ($m_b \geq 3.5$), from previous studies, together with eight solutions determined for this study (Annex 1), are shown in Figure 7 and listed in Table 2. Most solutions correspond to

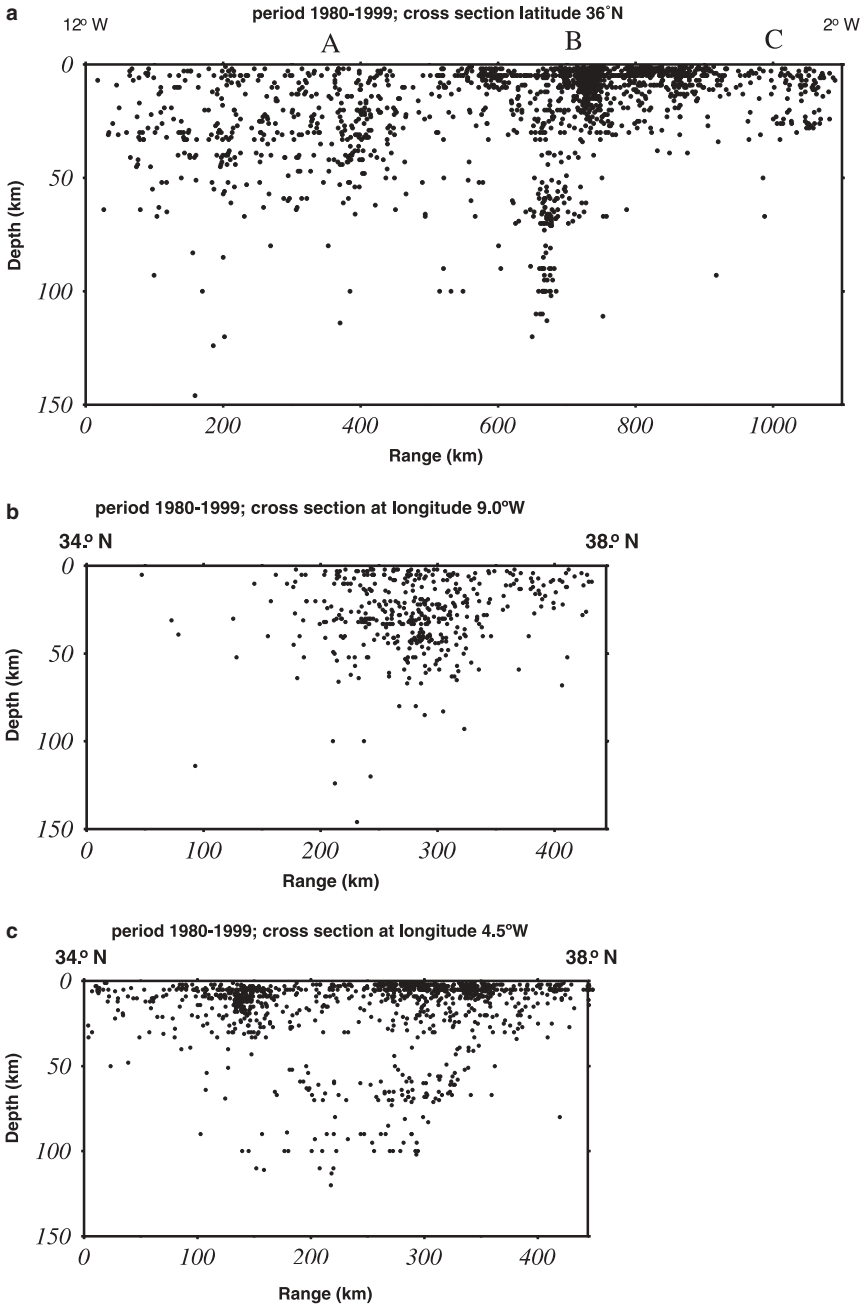

Figure 6
Vertical cross sections for the period 1980–1999 and magnitude greater than or equal to 3.5, (a) E-W section centered along 36°N, (b) N-S centered along 9°W and (c) NS centered along 4.5°W.

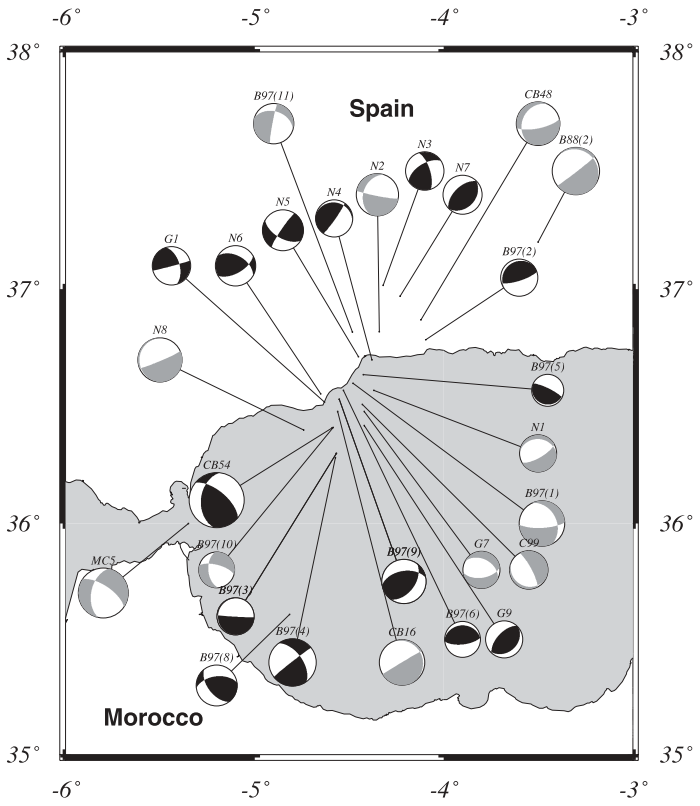

Figure 7
Focal mechanisms for intermediate depth earthquakes (40 < h < 150 km). Thrusting solutions in black and normal solutions in grey. Numbers correspond to Table 2.

earthquakes located very near the Spanish coast, where the concentration of epicenters is greater. Twelve of these solutions were obtained by modelling and inversion of body waves (Table 2) and the rest from first motion of *P* waves. Most solutions correspond to dip-slip motion, 7 to normal component and 9 to reverse component of motion. In most solutions the nearly vertical nodal plane has a mean orientation NE-SW. Only four shocks have an appreciable strike-slip component of motion. A nearly vertical tension axis has been obtained for 15 earthquakes (7 of them estimated from modelling or inversion of body waves).

Deep Earthquakes

An important feature of the seismicity of this region is the occurrence of very deep earthquakes at a depth of about 630 km. The largest of these earthquakes (M = 7) took place in 1954. These are the deepest earthquakes in the Mediterranean

Table 2

Solutions for focal mechanisms of intermediate depth earthquakes represented in Figure 7. ϕ: strike, :δ dip, *λ: slip. NF is the reference plotted with each solution*

Date	Lat. N.	Long.E	Depth	M	ϕ	δ	λ	NF	Ref.
130268	36.48	−4.56	91	4.3	334	10	5	CD16	3
130674	36.87	−4.12	60	4.1	78	72	−69	CB48	3
070875	36.41	−4.59	105	5.2	186	42	138	CB54	3
200679	37.20	−3.50	60	4.5	52	87	−102	B88(2)	4
220680	35.96	−5.23	81	4.7	304	76	−135	MC5	5
130586	36.60	−4.48	90	4.3	*87	74	−123	B97(1)	1
270387	36.79	−4.10	79	3.5	*69	72	76	B97(2)	1
300588	36.52	−4.63	80	3.6	75	88	35	G1	6
281188	36.30	−4.57	100	3.5	*93	88	−85	B97(3)	1
121288	36.28	−4.57	95	4.5	*232	87	146	B97(4)	1
190789	36.64	−4.43	95	3.0	*296	79	94	B97(5)	1
060290	36.57	−4.53	68	3.4	*270	23	96	B97(6)	1
130490	35.61	−4.82	89	3.9	*263	53	45	B97(8)	1
020590	36.53	−4.55	95	4.2	*36	49	57	B97(9)	1
181190	36.41	−4.59	85	3.4	*175	51	−30	B97(10)	1
250891	36.82	−4.48	58	3.8	*286	39	–173	B97(11)	1
140392	36.51	−4.43	64	3.6	*118	14	–123	C99	2
030992	36.48	−4.42	86	3.5	298	41	−61	G7	6
091193	36.42	−4.42	70	3.5	223	60	86	G9	6
010194	36.57	−4.37	68	3.5	60	71	–103	N1	7
170395	36.82	−4.34	56	4.0	100	85	−56	N2	7
181195	37.02	−4.32	52	3.6	238	59	154	N3	7
281195	36.70	−4.38	68	3.5	35	84	76	N4	7
220696	36.71	−4.45	68	3.9	120	58	172	N5	7
271296	36.56	−4.65	59	3.8	60	60	49	N6	7
180397	36.96	−4.23	56	3.7	43	34	87	N7	7
200897	36.40	−4.65	68	4.2	67	86	−63	N8	7

1. BUFORN *et al.* (1997); 2. COCA (1999); 3. COCA and BUFORN (1994); 4. BUFORN *et al.* (1988b); 5. MEDINA and CHERKAOUI (1992); 6. MORALES *et al.* (1999); 7. This paper; *wave-form modelling or inverison.

region and their origin is still an undecided question. During the period represented in Figure 2 very deep events occurred in 1990 and 1993 (Table 3). The 1990 event ($M_w = 4.8$) has been studied previously (BUFORN *et al.*, 1991b, 1997) and the 1993 earthquake, with a lower magnitude ($M_w = 4.4$), is studied in this paper (Annex 1). Their foci are located to the east of the concentration of the intermediate depth earthquakes at about the same location as that of the 1954 and 1973 events (CHUNG and KANAMORI, 1976; BUFORN *et al.*, 1991a, 1997). This occurrence of deep seismicity is concentrated in a very small area inland south of Granada, the east of the intermediate-depth seismicity that has most foci in the Alboran Sea. Focal mechanism solutions for deep earthquakes are all very similar (Fig. 8 and Table 3). Solutions have a vertical plane oriented N-S and the other nearly horizontal. Pressure and tension axes dip about 45°, with the pressure axis dipping to the east and the tension axis to the west. In this regard solutions differ from those for the

Table 3

Solution for focal mechanisms of deep depth earthquakes represented in Figure 8. ϕ: strike, δ: dip, λ: slip. NF is the reference plotted with each solutions

Date	Lat. N.	Long.E	Depth	M	ϕ	δ	λ	NF	Ref.
210354	37.00	−3.70	640	7.0	179	88	−122	B91(1)	1
300173	36.90	−3.70	660	4.8	191	74	−56	B91(2)	1
080390	37.00	−3.60	637	4.8	177	62	−91	B91(8)	1
310793	36.80	−3.43	663	4.4	177	60	−91	B02	2

1. Buforn *et al.* 1991a; 2. This paper

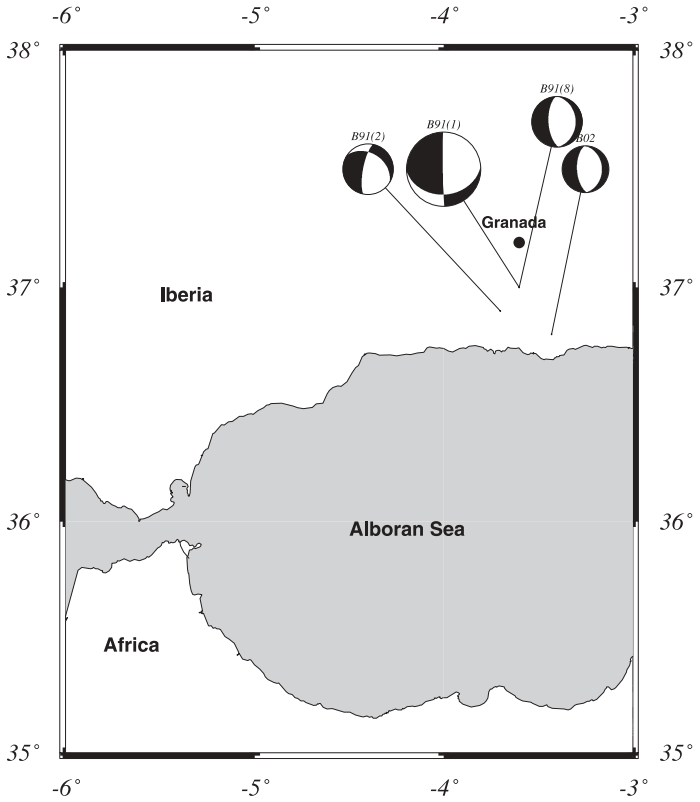

Figure 8
Focal mechanisms for very deep depth earthquakes (h > 600 km). Numbers correspond to Table 3

intermediate-depth earthquakes in which pressure axes dip to the south or southeast. From Figures 7 and 8 we observe, as a common characteristic of the focal mechanisms for intermediate-depth and very deep earthquakes, a nearly vertical plane. However the orientation of this plane is approximately E-W for intermediate shocks and N-S for the very deep ones.

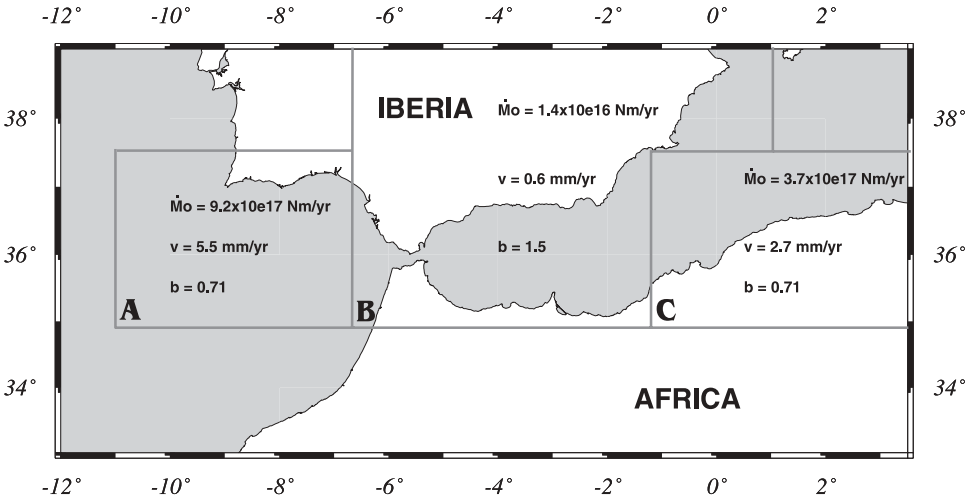

Figure 9
Moment rate, slip velocity and b values for the three studied areas (A, B and C).

Moment Rates, Slip Velocities and b Values

From the seismicity and focal mechanisms of shallow and intermediate-depth events, different behavior of the plate boundary in the three areas A, B and C from the Gulf of Cadiz to Algeria may be deduced. In order to quantify the characteristics of the seismicity in these three areas, the seismic moment rate, slip velocity and *b* value have been estimated for each of them. Results are shown in Figure 9. The moment rate was estimated from shallow earthquakes occurring in each area during the period 1900–1999 with magnitude $m_b \geq 5$. We used an empirical relation between magnitude m_b and scalar seismic moment M_o obtained from events with M_o values determined from spectra of body waves. The relation is similar to that obtained by other authors (BUFORN *et al.*, 1988a; EKSTRÖM and DZIEWONSKI, 1988; BADAL *et al.*, 2000).

$$\log \mathbf{M}_0 = 1.54\mathbf{m}_b + 8.7. \tag{1}$$

The moment rate M_0 was estimated by dividing the sum of the scalar seismic moment in each of the three areas by the time period (100 years).

Average slip velocity was estimated from the moment rate according to the expression

$$\Delta\dot{u} = \dot{M}_0/\mu S, \tag{2}$$

where μ is the rigidity coefficient and S the fault area. As an estimate of the slip velocity we used $\mu = 3 \times 10^4$ MPa, and for S we took the area of a vertical fault with a length of 550 km for parts A and B and 440 km for part C, and a width of 10 km

(the average depth for shallow shocks). This is equivalent to considering a fault with these dimensions as the origin of the shallow seismicity (Fig. 2).

The *b* values were obtained using earthquakes with magnitude $m_b \geq 3.0$ for the period 1950–1999. For this period the catalogue is considered complete for these magnitudes.

For areas A and C the same order of magnitude for the moment rate was obtained: 9.2×10^{17} Nm/yr for A and 3.7×10^{17} Nm/yr for C. These values are conditioned by the large earthquakes that occurred in area A in 1964 and 1969 and in area C in 1954 and 1980. However, for area B the moment rate (1.4×10^{16} Nm/yr) is nearly two orders of magnitude lower than that obtained for A and one order of magnitude lower than that for C. This is due to the fact that the maximum magnitude of earthquakes during the 20th century in area B is lower than 6 (largest shallow earthquake was $M_s = 5.1$ in 1951).

Values of slip velocity show similar results as those of moment rate: 5.5 mm/yr and 2.7 mm/yr for areas A and C and 0.6 mm/yr for area B. We have compared these results with the relative motions of Africa with relation to Eurasia predicted by the models NUVEL-1a (DeMets *et al.*, 1990) and DEOSK2 (Rui Fernandes, personal communication) (Table 4). These values have been estimated at the following points: 36.25°N, -8.5°W for area A; 37.0°N, −2.5°W for area B and 36.25°N, 1.25°E for area C. For area A, similar values are obtained in our study and by NUVEL-1a and DEOSK2 (Table 4), about 5 mm/yr in each case. For area C our velocity of 2.7 mm/yr is approximately 50% of the value obtained using NUVEL-1a and DEOSK2 models. However, the largest difference occurs in area B, where the velocity predicted by the models is very similar (5.2 mm/yr and 5.4 mm/yr, respectively) while our estimations give only 0.6 mm/yr, that is only about 10% of the modeled values. This may indicate that only a small fraction of the deformation was released seismically during the 20th century.

The *b* value for each area is as follows: in area B it is 1.5, and in both areas A and C it is 0.71. The difference in *b* values in areas A and C and area B corresponds to the different behavior of the seismic activity, with a large number of small to moderate earthquakes and an absence of large shocks in the last 50 years in area B, and larger earthquakes and a lower number of small ones in areas A and C.

Table 4

Values of slip velocity obtained from NUVEL 1a, DEOSK2 models and in this study

	NUVEL 1aa (mm/yr)	DEOSK2 (mm/yr)	This study
Gulf of Cadiz	4.3	5.0	5.5
Central region	5.2	5.3	0.6
Algeria	5.6	5.4	2.7

For intermediate-depth and deep earthquakes the moment rate, slip velocity and *b* values have not been estimated due to the low number of these earthquakes, for which depth determinations are reliable corresponding to recent years only.

In consequence, from Figure 9 we can conclude that in the Gulf of Cadiz and Algeria (areas A and C) the plate boundary between Eurasia and Africa corresponds to an area where the material is relatively rigid and the stresses are released by larger earthquakes. In the Betics, Alboran and Rif regions (area B) the material is more fragmented, with a large number of small faults, and consequently the stresses are released by frequent small to moderate earthquakes. As a consequence, the plate boundary is not well defined in area B and it corresponds to a wide area where deformation is manifested by the continuous occurrence of small earthquakes, and only occasionally, some moderate events occur. However, in the past, large events also have occurred in this area as shown by the historical seismicity (Fig. 3) and the lack of large earthquakes in the 1900–1999 period and the consequent low values of seismic moment rate and slip velocity may be due only to an anomalous period of seismic quiescence during the last century. In the 19th century at least two earthquakes (1829 and 1884) took place in southern Spain with magnitude greater than 6. For this region the time period selected (1900–1999) does not adequately represent the long range seismic activity of the region.

Frohlich Diagrams and Total Moment Tensor

From the results of focal mechanisms for shallow earthquakes shown in Figure 4 and Table 1, the Frohlich diagrams (FROHLICH and APPERSON, 1992) and the total seismic moment tensor for the three areas have been estimated (Fig. 10). The Frohlich diagrams for areas A and C show that most solutions correspond to reverse faulting, with only three mechanisms of pure strike-slip in area A and five in area C. A single solution corresponding to a normal motion is found in area A and there is a total absence of this type of faulting in area C. In area B the stress regime is more complex, strike-slip is the predominant motion and with a large component of normal and reverse faulting. A normal component is most frequent; it is present in 18 cases while reverse component is only present in 10 cases. Five mechanisms show pure normal faulting and four pure reverse faulting.

A problem in the use of the Frohlich diagrams is that in this representation all the earthquakes have the same weight, independent of their magnitude, and in consequence it is difficult to quantify the stress regime in an area. This may be solved with the use of the total seismic moment tensor defined as the sum of the moment tensors calculated from individual solutions:

$$M_{ij}^{\text{total}} = \sum_{k=1}^{N} M_0^k m_{ij}^k, \tag{3}$$

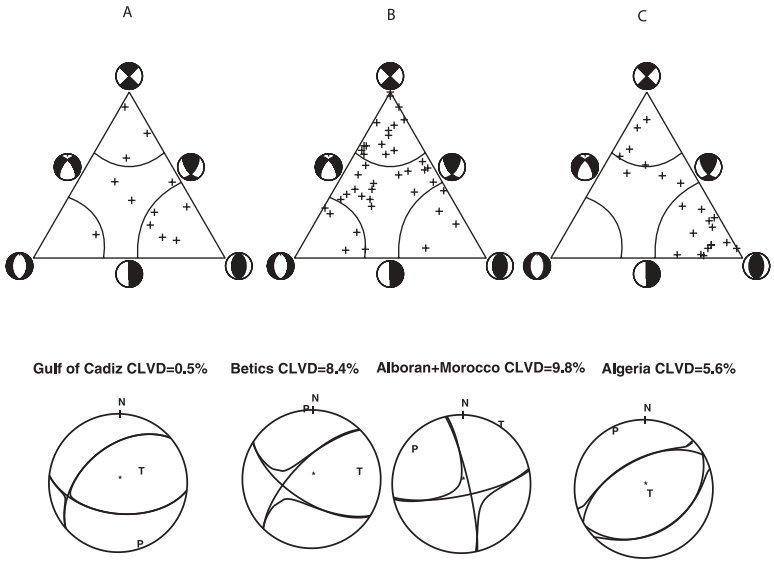

Figure 10
Frohlich diagrams and total seismic moment tensor for shallow earthquakes in the three studied regions. The CLVD component for each region is indicated.

where k is the number of earthquakes, M_0 the scalar seismic moment of each event and m_{ij} the seismic moment tensor components. Larger earthquakes (with high values of M_0) make a larger contribution in the estimation of the total seismic moment tensor. Equation (3) was used to estimate the components of total M_{ij} for the three regions using the solutions of Table 1. The total seismic moment tensor was separated into a DC and a non-DC (CLVD) component (DZIEWONSKI and WOODHOUSE, 1983). Results are shown in Figure 10. For area A (Fig. 10) the seismic moment tensor obtained corresponds to thrusting motion. This result is due to the solution of the 1969 earthquake. A similar result has been obtained for area C; the total seismic moment tensor shows thrusting motion due to the solutions of the earthquakes in the El Asnam region, especially that of the 1980 earthquake. The small non-DC components obtained (0.5% and 5.6%, respectively) confirm that solutions obtained for both regions are very similar and that large earthquakes control the stress regime in areas A and C.

In order to obtain coherent results, for area B it was necessary to subdivide the region into two: one part corresponds to the Betics and the other to the Alboran Sea and Morocco. For the Betics the stress regime corresponds to strike-slip faulting with a component of reverse motion, with the pressure axis nearly horizontal and oriented in N-S direction. For Alboran and Morocco the total moment tensor shows strike-slip motion with a small component of normal motion and horizontal tension axis oriented in a NE-SW direction. The amount of non-DC component is 8.4% and

9.8% for the Betics and Alboran and Morocco, respectively. The non-DC values obtained for both parts of area B, each less than 15%, indicates that for these regions the total seismic moment tensor obtained can be considered to represent the stress regime in the area. Thus in the three areas (A, B and C) there is a common orientation of the pressure axis which is horizontal and trending N-S to NW-SE. The tension axis is nearly vertical in areas A and C, and nearly horizontal in B trending E-W to NE-SW.

A similar study has been carried out for the intermediate-depth events (Fig. 11). Frohlich's diagram shows that most of the mechanisms correspond to dip-slip solutions, with a greater component of reverse motions. Only three solutions correspond to pure normal motion while 10 correspond to reverse motion. About 12 solutions correspond to motion on a nearly vertical or horizontal plane. From the total seismic moment tensor, a solution is obtained with a steeply dipping plane oriented NW-SE and a near horizontal plane. The pressure axis is horizontal and trending to the NE and the tension axis is almost vertical, with a small dip to the SE. The amount of non-DC component (0.8%) indicates that the stress regime resulting from the focal mechanism solutions for the intermediate-depth events is fairly uniform and may be represented by the solution shown in Figure 11.

For very deep earthquakes Frohlich's diagrams and the total seismic moment tensor have not been estimated. The reason is the small number (only four earthquakes) of similar solutions of focal mechanism and the large magnitude of the

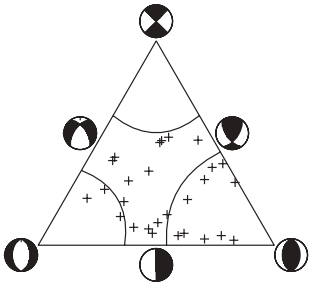

Figure 11
Frohlich diagrams and total seismic moment tensor for intermediate depth earthquakes in the Alboran region, the CLVD component is indicated.

1954 earthquake. In this case the total seismic moment tensor is controlled by the largest event, with $M = 7$, versus values of less than 5 for the other three earthquakes.

Seismotectonic Interpretation

Figure 12 depicts a proposed seismotectonic scheme for the studied region. The area delimited by the epicenters of shallow earthquakes (enclosed by the dashed lines) represents the surface expression of the plate boundary. In areas A and C (Gulf of Cadiz and Algeria regions) the plate boundary corresponds to a narrow band well defined by the seismicity, where large earthquakes ($M > 7$) occur in association with horizontal compression N-S to NNW-SSE due to the convergence of Eurasia and Africa. The intermediate-depth earthquakes, with a distribution in the E-W direction and delimited by a narrow band less than 20-km wide that broadens as we move to the Strait of Gibraltar, may also be associated with the convergence process of the

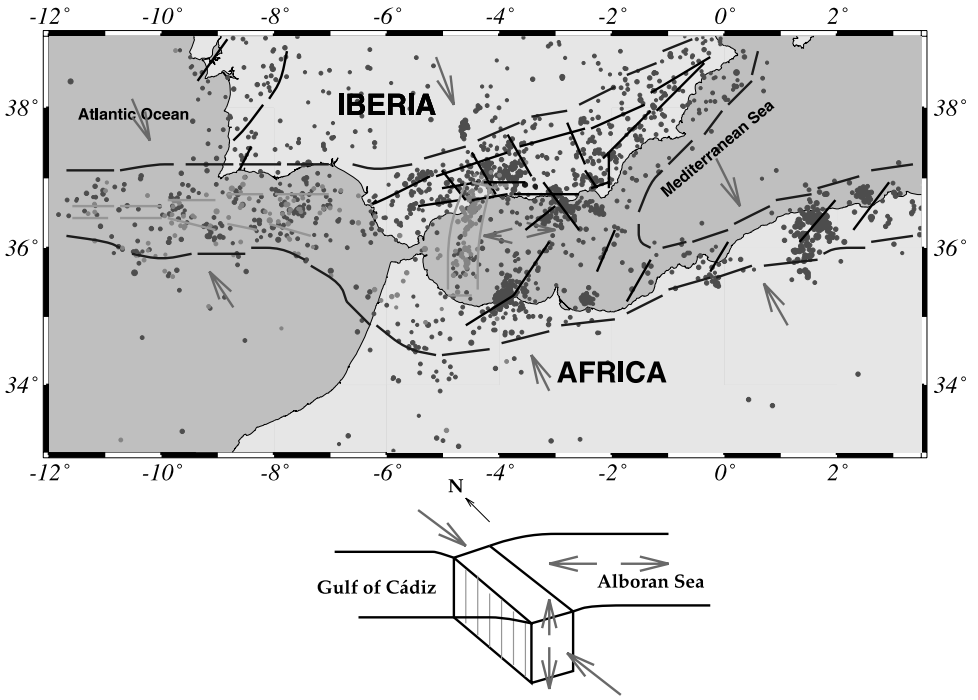

Figure 12
Seismotectonic scheme for the Iberia-Africa region. Shallow earthquakes are plotted in dark, intermediate depth events in grey. Arrows indicate the surface stress regime obtained from focal mechanisms of earthquakes. At bottom the seismogenic block proposed as origin of the intermediate depth seismicity at the western part of Alboran Sea.

Eurasia-Africa plates. No intermediate-depth earthquakes have been observed in the eastern part of the region (area C).

In area B the plate boundary is more diffuse and corresponds to a wider area that includes the Betics, the Alboran Sea and the Rif. It is difficult in this case to identify a simple line that corresponds to the plate boundary. In area B results of moment rate, slip velocity and *b* values indicate that the strain accumulated in the region is released partly in a continuous seismic activity of moderate magnitude over the whole area. Earthquakes with magnitudes larger than 6 occur at prolonged intervals. From historical seismicity it may be concluded that the 20th century was a period of anomalously low levels of seismic activity in this area. The stress regime obtained from the focal mechanisms of shallow events (Frohlich diagrams and total moment tensor) is compatible with horizontal N-S to NW-SE convergence of Eurasia and Africa. However in the Betics-Alboran area there is also a horizontal extension in an approximately E-W direction.

The existence of important seismic activity at intermediate depth (60 to 150 km) extending in a very narrow vertical band 50-km wide in N-S direction may be explained by the existence of a seismogenic block, of approximate dimensions 200-km long, 150-km deep and 50-km wide, on the eastern side of the Strait of Gibraltar. Inside this block the stress regime, deduced from focal mechanisms of earthquakes, corresponds to nearly vertical tension dipping to the SE. Different tectonic models have been proposed for this region, such as some kind of subduction process (BUFORN *et al*., 1988b, 1991a; MORALES *et al*., 1999), extensional collapse of thickened continental lithosphere (PLATT and VISSERS, 1989; HOUSEMAN, 1996), continental lithospheric delamination (DOCHERTY and BANDA, 1995; MÉZCUA and RUEDA, 1996; SEBER *et al*., 1996; CALVERT *et al*., 2000), backarc extension caused by subduction rollback (MORLEY, 1993; LONERGAN and WHITE, 1997; MICHARD *et al*., 2002), convective thinning (HOUSEMAN, 1996) or subduction and breaking of a slab of material (ZECK, 1996). Some of these models, such as continental lithospheric delamination, are not compatible with the presence of the intermediate-depth earthquakes and their focal mechanisms. The results presented here are consistent with the model presented by BUFORN *et al*. (1997) of an almost vertical slab of material with strike N-S driven by the extensional E-W forces present on the Alboran Sea, and under NW-SE compressive forces. The slab is being stretched downward, possibly by gravitational instability processes. Models which propose very low angle subduction or delamination (CALVERT *et al*., 2000) are not compatible with the results presented in this paper, due to the vertical distribution of hypocenters. Whatever explanation is given for the tectonics of this region, it must satisfy the geometry of the location of hypocenters and their focal mechanisms. Tomographic studies in this area show the existence of low velocity in the upper mantle between the Betic Cordillera and the Alboran Sea (SERRANO *et al*., 1998; MORALES *et al*., 1999). This anomaly is located in the western part of the Alboran Sea and it extends to 100-km depth, in the same region where the intermediate-depth events occur.

The presence of the very deep earthquakes (650 km) under southern Spain is a further sign of the complexity of area B. Their focal mechanisms correspond to pressure and tension axes trending E-W and dipping about 45°. Tomographic studies of the area show the existence of an anomalous high velocity region extending in depth from 200 km to 700 km (BLANCO and SPAKMAN, 1993). Only a very small part of the area, a volume where the foci are located, is seismically active. The relation of this deep activity with that of intermediate depth is not clear, but results of focal mechanisms and tomographic studies suggest different origins for them. In both cases these may be related to subduction processes, more recent for intermediate-depth shocks and older for very deep activity.

Acknowledgements

The authors wish to thank the Instituto Geográfico Nacional (Madrid, Spain) for providing part of the data. The authors also appreciate valuable comments and discussion given by Dr. D. McKnight. This work has been supported in part by the Ministerio de Ciencia y Tecnología (Spain), project REN2000-0777-C02-01.

REFERENCES

ARGUS, D., GORDON, R., DEMETS, C., and STEIN, S. (1989), *Closure of the Africa-Eurasia-North America Plate Motion Circuit and Tectonics of the Gloria Fault*, J. Geophys. Res. *94*, 5585–5602.

BLANCO, M.J. and SPAKMAN, W. (1993), *The P Velocity Structure of the Mantle below the Iberian Peninsula: Evidence for Subducted Lithosphere below South Spain*, Tectonophysics *221*, 13–43.

BADAL, J., SAMARDJIEVA, E., and PAYO, G. (2000), *Moment Magnitudes for Early (1923–1961) Instrumental Iberian Earthquakes*, Bull. Seismol. Soc. Am *90*,1161–1173.

BEZZEGHOUD, M. and BUFORN, E. (1999). *Source Parameters of the 1992 Melilla (Spain, $M_w = 4.8$), 1994 Alhoceima (Morocco, $M_w = 5.8$) and 1994 Mascara (Algeria, $M_w = 5.7$) Earthquakes and Seismotectonic Implications*, Bull. Seismol. Soc. Am. *89*, 359–372.

BOLETÍN DE SISMOS PRÓXIMOS (1989), Instituto Geográfico Nacional, Madrid.

BORGES, J.F., FITAS, A., BEZZEGHOUD, M., and TEVES-COSTA, P. (2001), *Seismotectonics of Portugal and its adjacent area*, Tectonophysics *337*, 373–387.

BUFORN, E., UDÍAS, A., and COLOMBÁS, M.A. (1988a), *Seismicity, Source Mechanisms and Seismotectonics of the Azores-Gibraltar Plate Boundary*, Tectonophysics *152*, 89–118.

BUFORN, E., UDÍAS, A., and MÉZCUA, J. (1988b), *Seismicity and Focal Mechanisms in South Spain*, Bull. Seismol. Soc. Am. *78*, 2008–2224.

BUFORN, E., UDÍAS, A., and MADARIAGA, R. (1991a), *Intermediate and Deep Earthquakes in Spain*, Pure Appl. Geophys. *136*, 375–393.

BUFORN, E., UDÍAS, A., MÉZCUA, J., and MADARIAGA, R. (1991b), *A deep Earthquake under South Spain, 8 March 1990*, Bull. Seismol. Soc. Am. *81*, 1403–1407.

BUFORN, E., SANZ DE GALDEANO, C., and UDÍAS, A. (1995), *Seismotectonics of the Ibero-Maghrebian Region*, Tectonophysics *248*, 247–261.

BUFORN, E., COCA, P., UDÍAS, A., and LASA, C. (1997), *Source Mechanism of Intermediate and Deep Earthquakes in Southern Spain*, J. Seism. *1*, 113–130.

BUFORN, E. and SANZ DE GALDEANO, C. (2001), *Focal Mechanism of Mula (Murcia, Spain) Earthquake of February 2, 1999*, J. Seism. *5*, 277–280.

CALVERT, A., GOMEZ, F., SEBER, D., BARAZANGI, M., JABOUR, N., IBENBRAHIM, A., and DEMNATI (1997), *An Integrate Geophysical Investigation of Recent Seismicity in the Al-Hoceima Region of North Morocco*, Bull. Seismol. Soc. Am. *87*, 637–651.

CHUNG, W. and KANAMORI, H. (1976), *Source Process and Tectonic Implications of the Spanish Deep-focus Earthquake of March 29, 1954*, Phys. Earth and Plan. Int. *13*, 85–96.

COCA, P. and BUFORN, E. (1994), *Mecanismos focales en el sur de España: periodo 1965–1985*, Estudios Geológicos, Madrid *50*, 1–2, 33–45.

COCA, P. (1999), *Métodos para la inversión del tensor momento sísmico. Terremotos del Sur de España*, Ph.D. Thesis, Universidad Complutense, Madrid, 300 pp.

DEMETS, C., GORDON, R., ARGUS, D., and STEIN, S. (1990), *Current Plate Motions*, Geophys. J. Int. *101*, 425–478.

DOCHERTY, C. and BANDA, E. (1995), *Evidence of Eastward Migration of the Alboran Sea Based on Regional Subsidence Analysis: A Case for Basin Formation by Delamination of Subcrustal Lithosphere?* Tectonics *14*, 430–433.

DZIEWONSKI, A. and WOODHOUSE, J. (1983), *An Experiment in Systematic Study of Global Seismicity: Centroid Moment Tensor Solutions*, J. Geophys. Res. *84*, 3247–3271.

EKSTRÖM, G. and DZIEWONSKI, A. (1988), *Evidence in on Bias in Estimations of Earthquakes Size*, Nature *332*, 319–323.

FROHLICH, C. and APPERSON, K.D. (1992), *Earthquake Focal Mechanisms, Moment Tensors and Consistency of Seismic Activity near Plate Boundaries*, Tectonics *11*, 279–296.

GRIMISON, N. and CHENG, W. (1986), *The Azores-Gibraltar Plate Boundary: Focal Mechanisms, Depths of Earthquakes and their Tectonic Implications*, J. Geophys. Res. *91*, 2029–2047.

HATZFELD, D. (1978), *Etude sismotectonique de la zone de collision Ibero-Maghrébine*, Ph.D. Thesis, Grenoble (France), 281 pp.

HAYWARD, N., WATTS, A.B., WESTBROOK, G.K. and COLLIER, J.S. (1999), *A Seismic Reflection and GLORIA Study of Compressional Deformation in the Gorringe Bank Region, Eastern North Atlantic*, Geophys. J. Int. *138*, 831–850.

HOUSEMAN, G. (1996), *From Mountains to Basin*, Nature *379*, 771–772.

JIMENEZ-MUNT, I., BIRD, P., and FERNANDEZ, M. (2001), *Thin-shell Modeling of Neotectonics in the Azores-Gibraltar Region*, Geophys. Res. Lett. *28*, 6, 1083–1086.

LAMMALI, K., BEZZEGHOUD, M., OUSSADOU, F., DIMITROV, D., and BENHALLOU, H. (1997), *Postseismic Deformation at El Asnam (Algeria) in the Seismotectonic Context of Northwestern Algeria*, Geophys. J. Int. *129*, 597–612.

LONERGAN, L. and WHITE, N. (1997), *Origin of the Betic-Rif Mountain Belt*, Tectonics *16*, 3, 504–522.

MCKENZIE, D. (1972), *Active Tectonics of the Mediterranean Region*, Geophys. J. R. Astron. Soc. *30*, 109–185.

MEDINA, F. and CHERKAOUI, T.E. (1992). *Mechanismes au foyer des seismes de Maroc et des régions voisines (1959–1986), Conséquences tectoniques*, Eclogae Geol. Helv. *85*, 433–457.

MÉZCUA, J. and MARTÍNEZ SOLARES, J.M. (1983), *Sismicidad del área Ibero-Mogrebí*, Instituto Geográfico Nacional Madrid.

MÉZCUA, J. and RUEDA, J. (1997), *Seismological Evidence for a Delamination Process in the Lithosphere under Alborán Sea*, Geophys. J. Int. *129*, F1–F8.

MICHARD, A., CHALOUAN, A., FEINBERG, H., GOFFÉ, B., and MONTIGNY, R. (2002), *How Does the Alpine Belt End between Spain and Morocco?* Bull. Soc. Geol. France *173*, 3–15.

MOKRANE, A., AIT MESSAOUD, A., SEBAI, A., MENIA, N., AYADI, A., BEZZEGHOUD, M. (1994), *Les séismes en Algérie de 1365 à 1992*, Bezzeghoud, M. and Benhallou, H. (eds). Publication du CRAAG, Alger-Bouzaréah, 277 pp.

MORALES, J., SERRANO, I., JABALOY, A., GALINDO-ZALDIVAR, J., ZHAO, D., TORCAL, F., VIDAL, F., and GONZALEZ-LODEIRO, F. (1999), *Active Continental Subduction beneath the Betic Cordillera and the Alboran Sea*, Geology *27*, 735–738.

MOREL, J. and MEGHRAOUI, M. (1996), *Gorringe-Alboran-Tell Tectonic Zone: A Transpressio System along the Africa-Eurasia Plate Boundary*, Geology *24*, 755–758.

MORLEY, C. (1993), *Discussion of the Origins of Hinterland Basins to the Rif-Betic Cordillera and Carpathians*, Tectonophysics *226*, 359–376.

MUNUERA, J.M. (1963), *Datos básicos para un estudio de sismicidad en la región de la Península Ibérica*. Mem. Inst. Geog. Cat., Madrid, 32, 93 pp.

MUÑOZ, D. and UDÍAS, A. (1988), *Evaluation of damage and source parameters of the Málaga earthquake of 9 October 1680*. In W.H.K. Lee, H. Meyer and K. Shimazaki, (eds), *Historical Seismograms and Earthquakes of the World* (Academic Press, San Diego 1988), pp. 208–221.

NEGREDO, A., BIRD, P., SANZ DE GALDEANO, C., and BUFORN, E. (2002), *Neotectonic Modeling of the Ibero-Maghrebian Region*, J. Geophys. Res., in press.

PLATT, J.P. and VISSERS, R. (1989), *Extensional Collapse of Thickened Continental Lithosphere: A Working Hypothesis for the Alboran Sea and Gibraltar Arc*, Geology *17*, 540–543.

RUEDA, J., MÉZCUA, J., and SANCHEZ RAMOS, M. (1996), *La serie sísmica de Adra (Almeria) de 1993–1994 y sus principales consecuencias sismotectónicas*, Avances en Geofísica y Geodesia, Instituto Geográfico Nacional, Madrid, 91–98.

SEBER, D., BARAZANGI, M., IBENBRAHIM, and DEMNATI, A. (1996), *Geophysical Evidence for Lithospheric Delamination beneath the Alboran Sea and Rif-Betic Mountains*, Nature *379*, 785–790.

SERRANO, I., MORALES, J., ZHAO, D., TORCAL, F., and VIDAL, F. (1998), *P-wave Tomographic Images in the Central Betics-Alboran Sea (South Spain) Using Local Earthquakes: Contribution for a Continental Collision*, Geophys. Res. Lett. *25*, 4031–4034.

TEJEDOR, J.M. and GARCÍA , O. (1993), *Funciones de transferencia de las estaciones de la red Sísmica Nacional*. Instituto Geográfico Nacional, Madrid, 82 pp.

TORNÉ, M., FERNANDEZ, M., COMAS, M.C., and SOTO, J.I. (2000), *Lithospheric Structure beneath the Alboran Basin: Results from 3D Gravity Modeling and Tectonic Revelance*, J. Geophys. Res. *105*, 3209–3228.

UDÍAS, A., LÓPEZ ARROYO, A., and MÉZCUA, J. (1976), *Seismotectonics of the Azores-Alboran Region*, Tectonophysics *31*, 259–289.

YELLES-CHAOUCHE, A.K., DJELLIT, H., BELDJOUDI, H., BEZZEGHOUD, M. and BUFORN, E, *The Ain Temouchent Earthquake of December 22th, 1999*, Pure Appl. Geophys., this issue.

ZECK, H. (1996), *Betic-Rif Orogeny: subduction of Mesozoic Tethys under E-ward Drifting Iberia, Slab Detachment Shortly before 22 Ma and Subsequent Uplift and Extensional Tectonics*, Tectonophysics *254*, 1–16.

(Received May 3, 2002, revised November 5, 2002, accepted December 12, 2002)

Annex 1

Focal mechanisms of earthquakes studied in this paper obtained from polarities of P-waves. At top date of the shock, black circles correspond to compressions and white circles to dilatations. T and P indicate the tension and pressure axis.

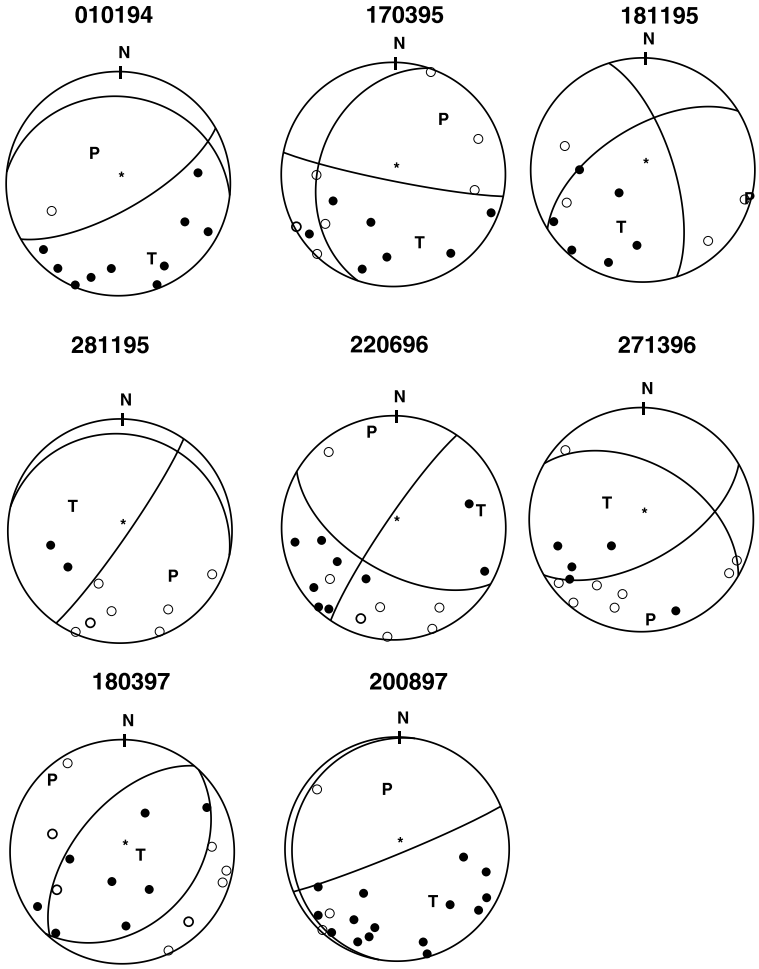

Annex 2